

Robot Iterative PD Optimization Control Algorithm and Offline VR Verification

Wenping Jiang^{1*}, Yijie Sun¹, Jin Liang¹, Weidong Du¹, Jun Min²

¹ School of Electrical and Electronic Engineering, Shanghai Institute of Technology, Shanghai, China

² School of Electrical and Electronic Engineering, Tongji University, Shanghai, China

*Corresponding Author.

Abstract:

Aiming at the problem that many industrial robot control algorithms only stay in theoretical simulation and mathematical model verification, and rarely realize verification in the actual industrial environment, in order to effectively verify the effectiveness and safety of the robot control algorithm in the actual industrial environment, this paper proposes a novel research method that combines industrial robot control algorithms with offline VR simulation verification. First, build the robot kinematics model, and design the iterative PD optimization control algorithm of the robot. According to the error between the actual trajectory and the expected trajectory, the algorithm adjusts the control amount, speed and joint angle of each joint by iteratively optimizing the PD parameters. Experiments show that after continuous iterative optimization, the error between the actual trajectory of the robot end and the expected trajectory is continuously reduced. When the number of iterations reaches 90, the error between the expected trajectory of the robot end and the actual trajectory is reduced to 0.001m. Secondly, the robot terminal trajectory obtained by the algorithm is imported into the offline VR environment of the robot, and the control algorithm is verified by spraying paint on the water pipe as an example. In the offline VR simulation process, the robot did not collide, the position was reachable, and the entire simulation was successfully completed, thus verifying the feasibility of the algorithm in the actual industrial environment.

Keywords: Iterative PD optimization control algorithm, robot kinematics, tracking, robot offline programming, spray paint, offline VR simulation

I. INTRODUCTION

With the rapid development of economy and society, the competition in the world's manufacturing industry has become increasingly fierce, and modern industry has put forward higher requirements for the productivity of the manufacturing industry. Due to the differences in the performance of domestic and foreign robots, foreign industrial robots account for more than 80% of the Chinese market in the precision operation of robots, while domestic robots can generally only be used in simple industrial scenarios such as loading, unloading and handling[1-3]. Therefore, for advanced control algorithms, it is necessary to go

through a set of effective industrial robot verification methods in order to put them into the actual industry more quickly, thereby improving productivity and work efficiency. At present, the control algorithms used in industrial robots mainly include traditional PID control methods, robust adaptive control algorithms, neural network control methods, sliding-mode control methods, etc. [4-7]. [8, 9] use iterative learning algorithms, combined with actual engineering conditions, to study the manipulator trajectory tracking problems. [10] proposes a research method that combines iterative learning with robust adaptive sliding mode control, which performs well in the presence of interference and uncertainty conditions. [11] proposes an intelligent predictive control method, uses neural network intelligent predictive controller to control the position and trajectory of the robot. The controller of neural network can approach the uncertain conditions of the industrial robot without knowing the exact structure of the system. [12] analyzed the stability of the robot system, then, the PID controller is corrected, the parameter values of K_p , T_i and T_d are set by Ziegler-Nichols method, the transfer function of PID controller is obtained, then, the complex system function is calculated.

In the aspect of industrial robot algorithm verification, scholars have also proposed various methods. [13] proposes a novel method—Dynamic Environment Rapid Search Tree, the method is demonstrated on the robot under real environment. [14] presents a novel calibration method for joint-dependent geometric errors based on 6-DOF industrial robots. Chebyshev polynomials are used to characterize the intricacy joint-dependent geometric error model, revealing the impact of strain wave gearing errors and other sources more correctly. [15-20] use the mathematical verification method: Lyapunov function, to verify the stability of the robot control system. [21] presented a 7-DOF parallel hybrid humanoid robotic arm, compared with another commonly-used trajectory planning methodology, the effectiveness and feasibility of the proposed methodology are verified through numerical simulations.

From the above paper [13-21], it is not difficult to find that most of the robotic arm algorithm verification still uses traditional mathematical methods such as Lyapunov equation, or directly simulates the algorithm in the real environment on the robotic arm. Among them, the former method can only theoretically judge the stability of the control system, but cannot determine whether the algorithm is feasible in the actual industrial environment; the latter method has verified the feasibility of the algorithm in the actual environment, but from the perspective of safety, when a new algorithm is simulated for the first time, there will often be a lot of uncertainty and security risks. Based on this, this paper proposes a novel research method that combines the robotic arm control algorithm with offline VR simulation technology. First, design the robot mechanical model and establish the robot kinematics equation; secondly, through iterative PD optimization control algorithm and kinematic model, with iteration, the actual tracking trajectory of the robot is obtained; finally, the actual trajectory and model of the robot are imported into the robot offline VR simulation software, the VR painting operation of the spiral water pipe by the robot is realized to verify the feasibility of the algorithm in an industrial environment.

II. BACKGROUND AND METHODS

The research object of the experiment in this paper is based on a three-degree-of-freedom robot modeled by SOLIDWORKS. The length of the robot base $a_1=0.6\text{m}$; the length of the first arm $a_2=0.6\text{m}$ and the second arm $a_3=0.4\text{m}$. The 3D model of the three-degree-of-freedom robot is shown in Figure 1:

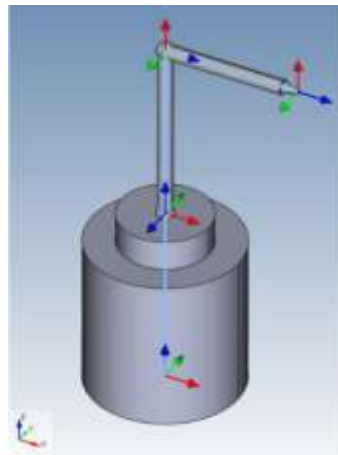


Fig 1: 3D model of three-degree-of-freedom robot

2.1 Robot Kinematics Modeling

The D-H parameters of the three-degree-of-freedom robot are shown in Table 1.

TABLE I. Three-degree-of-freedom robot D-H parameters

No.	Joint	$\theta(^{\circ})$	$d(\text{m})$	$a(\text{m})$	$\alpha(^{\circ})$
1	BASE+J1	θ_1	$0.1+0.5$	0	0
2	J2	θ_2	0	0.6	90
3	J3	θ_3	0	0.4	0

The transformation matrix of the robot from the base to the end effector can be described as:

$${}^0T_3 = A_1 A_2 A_3 \quad (1)$$

Where:

$$A_n = \begin{bmatrix} \cos \theta_n & -\sin \theta_n \cos \alpha_n & \sin \theta_n & a_n \cos \theta_n \\ \sin \theta_n & \cos \theta_n \cos \alpha_n & -\cos \theta_n \sin \alpha_n & a_n \sin \theta_n \\ 0 & \sin \alpha_n & \cos \alpha_n & d_n \\ 0 & 0 & 0 & 1 \end{bmatrix} \quad (2)$$

Substituting the D-H parameters in Table 1 into the formula (2), we get:

$$A_1 = \begin{bmatrix} \cos \theta_1 & -\sin \theta_1 & \sin \theta_1 & 0 \\ \sin \theta_1 & \cos \theta_1 & 0 & 0 \\ 0 & 0 & 1 & 0.6 \\ 0 & 0 & 0 & 1 \end{bmatrix} \quad (3)$$

$$A_2 = \begin{bmatrix} \cos \theta_2 & 0 & \sin \theta_2 & 0.6 \cos \theta_2 \\ \sin \theta_2 & 0 & -\cos \theta_2 & 0.6 \sin \theta_2 \\ 0 & 1 & 0 & 0 \\ 0 & 0 & 0 & 1 \end{bmatrix} \quad (4)$$

$$A_3 = \begin{bmatrix} \cos \theta_3 & \sin \theta_3 & \sin \theta_3 & 0.4 \cos \theta_3 \\ \sin \theta_3 & -\cos \theta_3 & 0 & 0.4 \sin \theta_3 \\ 0 & 0 & -1 & 0 \\ 0 & 0 & 0 & 1 \end{bmatrix} \quad (5)$$

Substitute formulas (3), (4), and (5) into formula (1) to obtain the total transformation matrix of the three-degree-of-freedom manipulator.

The geometric relationship diagram of the three-degree-of-freedom manipulator model is shown in Figure 2:

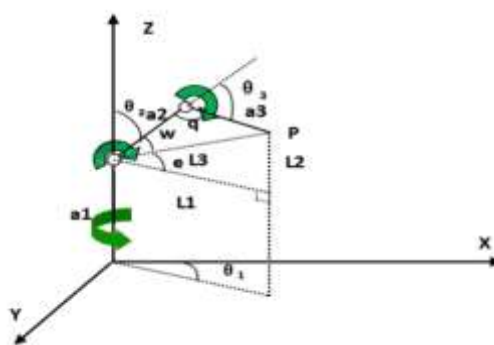


Fig 2: Geometric model of manipulator

Suppose the end of the manipulator is point P (X, Y, Z). The lengths of L1, L2, and L3 are:

$$\begin{cases} L_1 = \sqrt{X^2 + Y^2} \\ L_2 = Y - a_1 \\ L_3 = \sqrt{L_1^2 + L_2^2} \end{cases} \quad (6)$$

Knowing the lengths of L_1 , L_2 , and L_3 , the angle values of the three angles q , w , and e can be calculated as follow:

$$\begin{cases} q = \arccos \frac{a_2^2 + a_3^2 - L_3^2}{2a_2a_3} \\ w = \arccos \frac{a_2^2 + L_3^2 - a_3^2}{2a_2L_3} \\ e = \arctan \frac{L_2}{L_1} \end{cases} \quad (7)$$

According to the robot kinematics, the angle values of θ_1 , θ_2 , and θ_3 can be described by formulas (6) and (7):

$$\begin{cases} \theta_1 = \arctan \frac{Y}{X} \\ \theta_2 = \frac{\pi}{2} - \arccos \frac{a_2^2 + L_3^2 - a_3^2}{2a_2L_3} - \arctan \frac{L_2}{L_1} \\ \theta_3 = \pi - \arccos \frac{a_2^2 + a_3^2 - L_3^2}{2a_2a_3} \end{cases} \quad (8)$$

2.2 Robot Iterative PD Optimal Controller

The Simulink of Iterative PD optimization controller for the three-degree-of-freedom manipulator is shown in Figure 3:

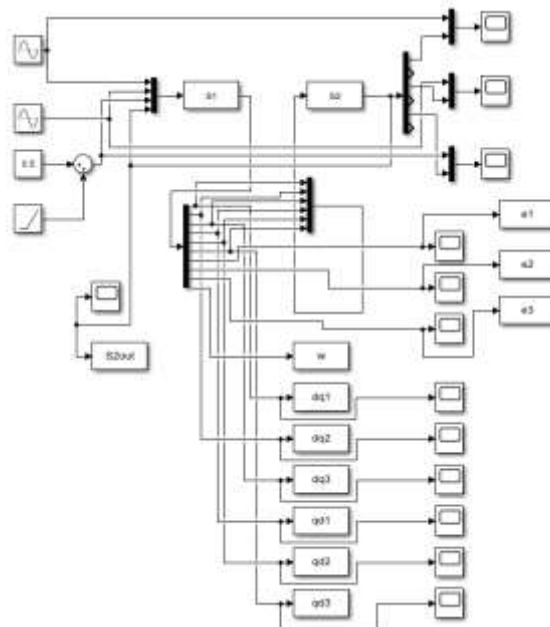


Fig 3: Three-degree-of-freedom robot Iterative PD optimized controller

The controller consists of three inputs, two S-functions and three outputs. The input is the desired trajectory of the end of the three-degree-of-freedom manipulator; the two S-functions are: Motion Controller S1 and controlled system S2; the output is the tracking of the actual trajectory. Among them: Motion Controller S1 is responsible for calculating the actual trajectory and actual end speed; Controlled system S2 is responsible for calculating the Kp and Td parameters based on the trajectory error e and the velocity error de . Then, using the Jacobian matrix and Robot kinematics, calculating the trajectory and the speed of the end of the manipulator at the next moment.

The mathematical models of two S-function will be introduced in chapter 2.2.1 & 2.2.2.

2.2.1 Mathematical model of motion controller S1

Define the desired trajectory as:

$$\begin{cases} R_x = 0.5 \sin(t) \\ R_y = 0.5 \cos(t) \\ R_z = 0.5 + 0.05(t) \end{cases} \quad (9)$$

Derivation to obtain the desired speed of the robot end on the X Y Z axis:

$$\begin{cases} V_x = 0.5 \cos(t) \\ V_y = -0.5 \sin(t) \\ V_z = 0.05 \end{cases} \quad (10)$$

Combining the data in formulas (9) and (10), according to the robot kinematics, the expected angles of the three joints are obtained:

$$\begin{cases} qd_1 = \arctan \frac{R_2}{R_1} \\ qd_2 = \arctan \frac{a_3 c(qd_3 + a_2) \cdot (R_1 - a_1) - a_3 s qd_3 \cdot R_1 c(qd_1 + R_2 s qd_1)}{(a_3 c qd_3 + a_2) \cdot (R_1 c qd_1 + R_2 s qd_1) + a_3 s qd_3 (R_3 - a_1)} \\ qd_3 = \arctan \frac{(R_1 c qd_1 + R_2 s qd_1)^2 + (R_3 - a_1)^2 - a_2^2 - a_3^2}{2 a_2 a_3} \end{cases} \quad (11)$$

Where qd_i is the expected angle of the three joints, a_i is the length of the three robotic arm, c is \cos and s is \sin .

The error matrix between the expected trajectory and the actual trajectory on the three coordinate axes is as follows:

$$e = \begin{bmatrix} e_1 \\ e_2 \\ e_3 \end{bmatrix} = \begin{bmatrix} R_1 - R_X \\ R_2 - R_Y \\ R_3 - R_Z \end{bmatrix} \quad (12)$$

In the same way, the error matrix between the expected speed and the actual speed on the three axes is as follow:

$$de = \begin{bmatrix} de_1 \\ de_2 \\ de_3 \end{bmatrix} = \begin{bmatrix} dr_1 - V_X \\ dr_2 - V_Y \\ dr_3 - V_Z \end{bmatrix} \quad (13)$$

The parameters K_p and T_d of the iterative PD optimization controller are two third-order matrixs, and the parameters m and n will change continuously with the number of iterations increases, so as to optimize the control amount under different combinations of K_p and T_d :

$$KP = \begin{bmatrix} m & 0 & 0 \\ 0 & m & 0 \\ 0 & 0 & m \end{bmatrix} \quad (14)$$

$$Td = \begin{bmatrix} n & 0 & 0 \\ 0 & n & 0 \\ 0 & 0 & n \end{bmatrix} \quad (15)$$

From formulas (12), (13), (14), (15), the control variables dq and the spatial error w of the three joints are obtained:

$$dq = \begin{bmatrix} dq_1 \\ dq_2 \\ dq_3 \end{bmatrix} = Kp \cdot e + Td \cdot de \quad (16)$$

$$w = \sqrt{e_1^2 + e_2^2 + e_3^2} \quad (17)$$

Among them, the spatial error reflects the tracking performance of the iterative PD optimization controller at each time node. The larger the spatial error, the worse the tracking performance at a certain time node.

2.2.2 Mathematical model of controlled system S2

The angle value matrix q of the three joints of the robot is obtained by adding the expected angles of the three joints and the control variables of the three joints of the iterative PD optimization controller:

$$q = \begin{bmatrix} q_1 \\ q_2 \\ q_3 \end{bmatrix} = \begin{bmatrix} qd_1 + dq_1 \\ qd_2 + dq_2 \\ qd_3 + dq_3 \end{bmatrix} \quad (18)$$

The Jacobian matrix J of the robot is:

$$J = \begin{bmatrix} -a_2s_1c_2 - a_3s_1(c_2 + c_3) & -a_2c_1s_2 - a_3c_1(s_2 + s_3) & -a_3c_1(s_1 + s_2) \\ a_2c_1c_2 + a_3c_1(c_2 + c_3) & -a_2s_1s_2 - a_3s_1(s_2 + s_3) & -a_3s_1(s_1 + s_2) \\ 0 & a_2s_1c_2 + a_3(c_2 + c_3) & a_3(c_2 + c_3) \end{bmatrix} \quad (19)$$

Where $a_2s_1c_2 = a_2\sin q_1 \cos q_2$ and so on.

According to the Jacobian matrix in formula (19) and the joint control value in formula (16), the real-time linear velocity of the robot end on the X, Y, and Z axes is calculated:

$$V = \begin{bmatrix} V_X \\ V_Y \\ V_Z \end{bmatrix} = J \cdot dq \quad (20)$$

From the robot kinematics, the simulation trajectory of the robot end effector on the X, Y, and Z axes is calculated:

$$R = \begin{bmatrix} R_X \\ R_Y \\ R_Z \end{bmatrix} = \begin{bmatrix} \cos q_1 \cdot [a_2 \cos q_2 + a_3 \cos (q_2 + q_3)] \\ \sin q_1 \cdot [a_2 \cos q_2 + a_3 \cos (q_2 + q_3)] \\ a_1 + a_2 \sin q_2 + a_3 \sin (q_2 + q_3) \end{bmatrix} \quad (21)$$

According to the expected trajectory in formula (9) and the actual trajectory in formula (21), we can observe the trajectory tracking of the robot end in the iterative PD optimization control algorithm. The error matrix in formula (19) and the spatial error in formula (17) reflect the trajectory tracking performance of the robot end. The iterative PD optimization control algorithm passes through multiple iterations, and the trajectory with the smallest error coefficient is used as the final trajectory tracking output.

III. EXPERIMENTS

3.1 Algorithm Simulation

The iterative PD optimization control algorithm is used for 90 iterations, and each iteration corresponds to a new set of PD parameters. In the experiment, the sampling frequency of the simulation is defined as 5Hz, so each iteration will generate 51 sets of data, and each iteration will produce a spatial error w in formula (17). The largest spatial error, w_{\max} , among 51 iterations is selected as our evaluation index. As the number of iterations increases, the optimization of the maximum spatial error w_{\max} is shown in Figure 4:

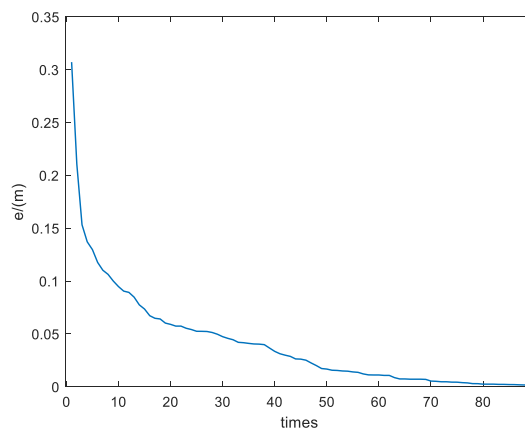


Fig 4: The relationship between the max spatial error w_{\max} and iterations

From formula (11), when the iteration reaches 90 times, the real-time joint angles of the robot's three joints are shown in Figure 5:

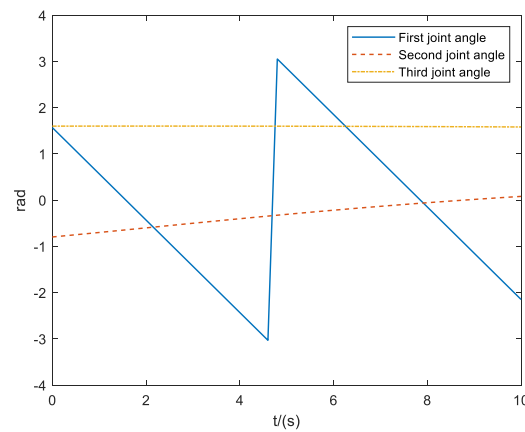


Fig 5: Real-time angle of three robot joints

From formula (20), when the iteration reaches 90 times, the speed of the robot end in space changes with time as shown in Figure 6:

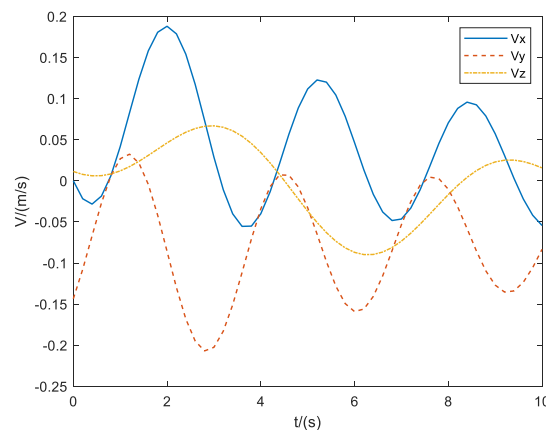
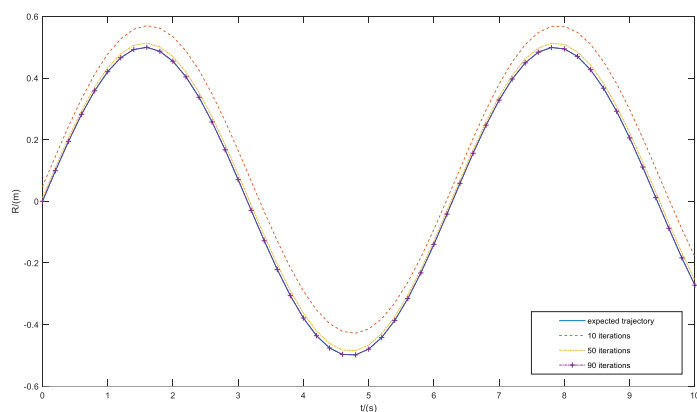
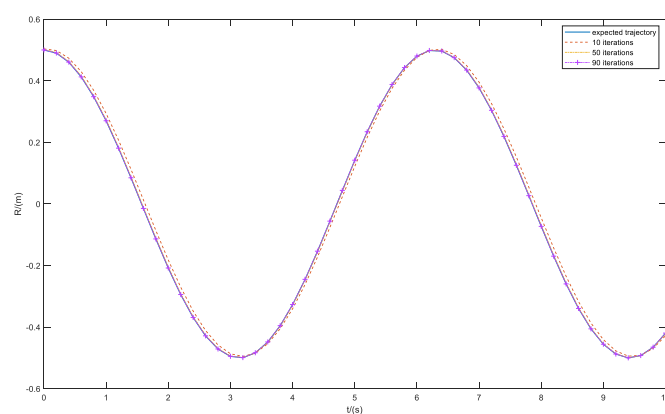


Fig 6: The speed of the end in space changes with time

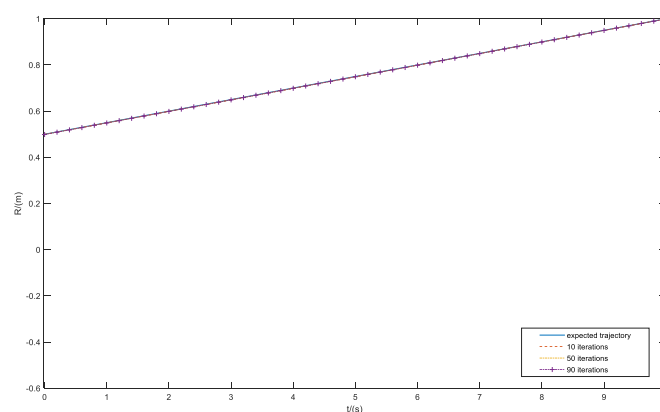
According to formula (21), after 10, 50, and 90 iterations by the iterative PD optimization controller, the trajectory of the robot end on the X, Y, and Z axes is compared with the expected trajectory so as to observe the impact of iteration on trajectory tracking, as shown in Figure 7 (a), (b), (c):



(a) Tracking curve on the x-axis



(b) Tracking curve on the y-axis



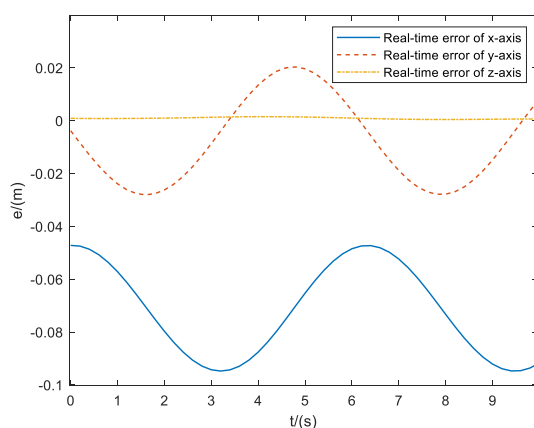
(c) Tracking curve on the z-axis

Fig 7: The effect of iteration on tracking performance

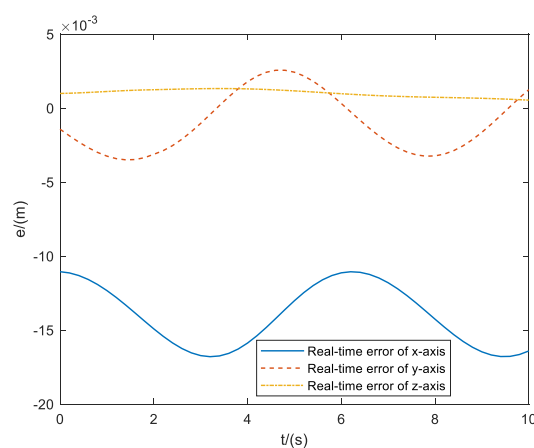
The parameters for 10 iterations in Figure 8 are: $K_p=440$, $T_d=0.7$; the parameters for 50 iterations are:

$K_p=450$, $T_d=0.5$; the parameters for 90 iterations are: $K_p=410$, $T_d=0.1$. From Figure 8 (a), (b), and (c), it can be observed that as the number of iterations increases, the actual trajectory on the 3-axis is constantly approaching the desired trajectory. When the number of iterations rises to 90, the actual trajectory and the expected trajectory almost overlap with minimal error; a good tracking effect is obtained.

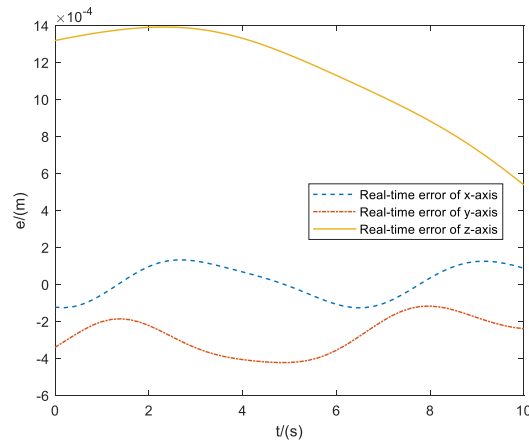
From formula (12), when iteration reaches 10, 50, and 90 times, the error between the expected trajectory of the robot end on the X, Y, and Z axis and the simulated trajectory is shown in Figure 8 (a), (b), (c):



(a) Error curve at 10 iterations



(b) Error curve at 50 iterations



(c) Error curve at 90 iterations

Fig 8: The error between the expected trajectory and the actual trajectory on the X, Y, and Z axes

This experiment was carried out on a HP notebook computer equipped with 8G memory and Intel Core i7-8750H processor, the experiment software is MATLAB R2018b. In summary, the table summarizes the performance of the iterative PD optimization control algorithm in all aspects of the trajectory tracking test, as shown in Table 2:

TABLE II. The performance of iterative PD optimization controller

NO.	Number of iterations	Parameters		Maximum error (m)	Average absolute error (m)	time cost (s)
		K_p	T_d			
1	10	440	0.7	0.09485	0.04849	5.03
2	50	450	0.5	0.01680	0.01404	18.37
3	90	410	0.1	0.00143	0.00114	32.22

3.2 Offline VR Verification

The experimental verification process of the algorithm (robot offline painting VR simulation) can be divided into four stages as follow:

- (1) Import robot model
- (2) mechanism definition

(3) Import each trajectory point in the algorithm and generate a trajectory

(4) Import the workpiece and start the virtual simulation

The robot model is shown in Figure 1. Secondly, define the mechanism for the robot. The mechanism definition includes 2 steps: D-H parameter setting and joint limit. The setting of DH parameters has been shown in Table 1. Joint limit is shown in Table 3:

TABLE III. Joint limit of manipulator

NO.	Joint	Mechanical zero (mm)	Maximum limit(°)	Minimum limit(°)	Movement direction
1	J1	0	360	-360	Positive
2	J2	0	75	-75	Positive
3	J3	0	75	-75	Positive

After completing mechanism definition, import each trajectory point generated by the algorithm after 90 iterations into the offline programming software in turn, as shown in Figure 9.

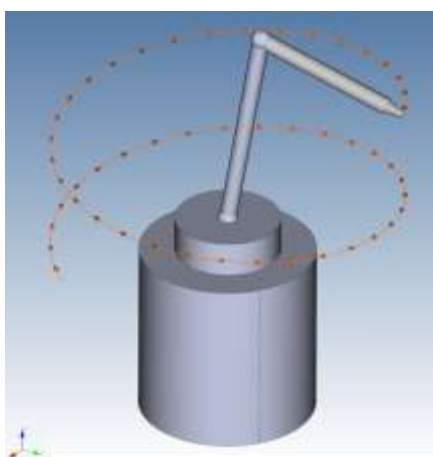
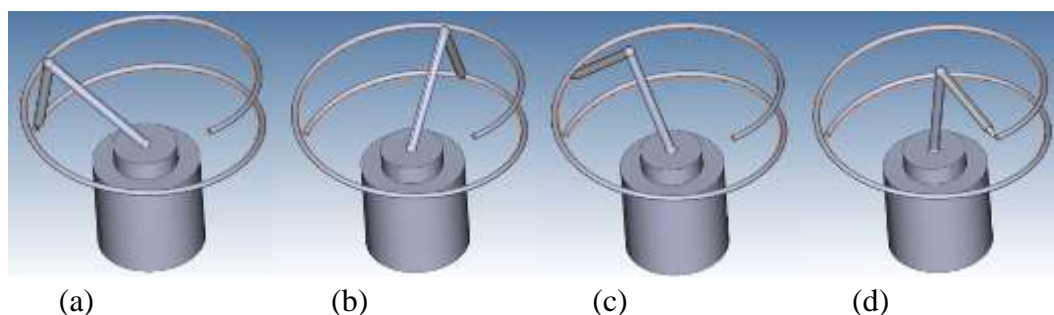


Fig 9: import trajectory points and generate trajectory

Finally, the trajectory obtained by the iterative PD optimization control algorithm after 90 iterations is imported into the robot offline programming environment, and the painting operation is performed in the offline environment for VR simulation. Throughout the simulation process, the end position of the robot was reachable, and there was no collision during the simulation process. The robot successfully completed the painting operation of the water pipe in the offline VR environment. The VR simulation process is

shown in Figure 10 (a), (b), (c), (d):



(a) The robot is ready to start simulation

(b) The end of the robot is at the 9th sampling point

(c) The end of the robot is at the 32nd sampling point

(d) Robot simulation is over

Fig 10: Robot spray paint experiment on water pipe in VR environment

IV. CONCLUSION

In this paper, an iterative PD optimization control algorithm based on a three-degree-of-freedom robot is designed, and the robot is modeled in kinematics. By designing the main program of the iterative PD optimization control algorithm, the motion Controller and the controlled object, the output experimental data is processed and analyzed. Experimental results show that when the number of iterations reaches 90 times, the actual trajectory of the robot end achieves a very good tracking effect relative to the expected trajectory. Finally, the robot end trajectory after 90 iterations is applied to the robot offline environment for VR painting simulation experiment. In the experiment, the position of the robot is reachable, there is no collision with the water pipe, and the entire painting simulation process is successfully completed. The kinematics model in this algorithm is completely independent from the kinematics model on the robot offline VR simulation software, and the same robot inverse solution is obtained, which fully proves the feasibility of the algorithm to be used in an industrial environment.

From a forward-looking perspective of industrial applications, the research method that combines industrial robot control algorithms with VR offline simulation not only ensures that advanced robot control algorithms can be quickly put into actual production, thereby improving industrial production efficiency, but also advanced control algorithm can be pre-simulated in offline VR software to ensure the safety and feasibility of the new algorithm in actual production.

ACKNOWLEDGEMENTS

This research was supported by Interdisciplinary and multi-field cooperative research special project of the Collaborative Innovation Fund (XTCX2021-10).

This research was supported by The Ministry of Education Industry-University-Research Cooperation Collaborative Education Project (201902025016).

REFERENCES

- [1] Qiu Zurong and Xue Jie. Review of performance testing of high precision reducers for industrial robots. Measurement, 2021, 183
- [2] Tang Chengjian and Huang Keqi and Liu Qiren. Robots and skill-biased development in employment structure: Evidence from China. Economics Letters, 2021, 205
- [3] Taylor Annalisa T. and Berrueta Thomas A. and Murphey Todd D. Active learning in robotics: A review of control principles. Mechatronics, 2021, 77
- [4] Souza Darielson A. et al. PID controller with novel PSO applied to a joint of a robotic manipulator. Journal of the Brazilian Society of Mechanical Sciences and Engineering, 2021, 43(8)
- [5] Shu-Huan Wen et al. Unactuated Force Control of 5-DOF Parallel Robot Based on Fuzzy PI. International Journal of Control, Automation and Systems, 2020, 18: 1-12.
- [6] Tie Zhang and Ye Yu and Yanbiao Zou. An Adaptive Sliding-Mode Iterative Constant-force Control Method for Robotic Belt Grinding Based on a One-Dimensional Force Sensor. Sensors, 2019, 19(7): 1635- 1635.
- [7] Song Ling, Huanqing Wang, Peter X. Liu. Adaptive Fuzzy Dynamic Surface Control of Flexible-Joint Robot Systems With Input Saturation. IEEE/CAA Journal of Automatica Sinica, 2019, 6(01): 97-107.
- [8] Kaloyan Yovchev. Finding the Optimal Parameters for Robotic Manipulator Applications of the Bounded Error Algorithm for Iterative Learning Control. Journal of Theoretical and Applied Mechanics, 2017, 47(4): 3-11.
- [9] Farah Bouakrif and Michel Zasadzinski. Trajectory tracking control for perturbed robot manipulators using iterative learning method. The International Journal of Advanced Manufacturing Technology, 2016, 87(5-8): 2013-2022.
- [10] Ehsan Ghotb Razmjou and Seyed Kamal Hosseini Sani and Jalil Sadati. Robust adaptive sliding mode control combination with iterative learning technique to output tracking of fractional-order systems. Transactions of the Institute of Measurement and Control, 2018, 40(6): 1808-1818.
- [11] Yini Wang. Robot algorithm based on neural network and intelligent predictive control. Journal of Ambient Intelligence and Humanized Computing, 2019: 1-12.
- [12] Xianxin Lin, Guojin Li, Qian Su, Xi Li. Research on Stability of Sand Core Handling Robot System Based on PID Control//Proceedings of 2021 The 2nd International Conference on Mechanical Engineering and Materials (ICMEM 2021)., 2021: 414-422. DOI:10.26914/c.cnkihy.2021.037839.
- [13] Zheng Xiaoliang and Wu Gongping. Kinodynamic planning with reachability prediction for PTL maintenance robot. Proceedings of the Institution of Mechanical Engineers, Part I: Journal of Systems and Control Engineering, 2021, 235(8): 1417-1432.
- [14] Jiang Zhouxiang et al. A new calibration method for joint-dependent geometric errors of industrial robot based on multiple identification spaces. Robotics and Computer-Integrated Manufacturing, 2021, 71
- [15] Shang Wei et al. A Distributed Model Predictive Control for Multiple Mobile Robots with the Model Uncertainty. Discrete Dynamics in Nature and Society, 2021, 2021
- [16] Zhen ShengChao et al. A new PD based robust control method for the robot joint module. Mechanical Systems and Signal Processing, 2021, 161

- [17] Liu Yu et al. Asymmetric Input-Output Constraint Control of a Flexible Variable-Length Rotary Crane Arm. IEEE transactions on cybernetics, 2021, PP
- [18] CruzOrtiz David and Chairez Isaac and Poznyak Alexander. Non-singular terminal sliding-mode control for a manipulator robot using a barrier Lyapunov function. ISA transactions, 2021.
- [19] PizarroLerma Andres et al. Sectorial Fuzzy Controller Plus Feed forward for the Trajectory Tracking of Robotic Arms in Joint Space. Mathematics, 2021, 9(6): 616-616.
- [20] Wang Zesheng et al. A multi-objective approach for the trajectory planning of a 7-DOF serial-parallel hybrid humanoid arm. Mechanism and Machine Theory, 2021, 165
- [21] Fan Yidi and Jing Wuxing. Inertia-free appointed-time prescribed performance tracking control for space manipulator. Aerospace Science and Technology, 2021, 117(pre-publish): 106896-.